PRELIMINARY ASSESSMENT ON THE DEVELOPMENT OF COST-COMPETITIVE PVA-FIBER REINFORCEMENT MORTAR

Esmaeel Esmaeeli

Joaquim António Oliveira de Barros

Delfina M. F. Gonçalves

Report 10-DEC/E-09

Date: June 2010

Number of pages: 30

Keywords: Engineered Cementitious Composites, Strain Hardening, Bending Test, Direct Tensile test

School of Engineering

Department of Civil Engineering

University of Minho

Azurém 4800-085 Guimarães

Table of contents

Tables

Figures

1 INTRODUCTION

Cementitious materials, such as concrete and mortar, exhibit brittle tensile behavior. However, their behavior can be significantly improved by adding discontinuous fibers [1]. Nowadays, several types of reinforcing fibers, in various shapes and sizes, such as steel, polymer, glass, carbon, or natural fiber, are produced and used widely. Recently, in order to minimize confusion, Naaman and Reinhardt [2] suggested the use of a classification which applies to all fiber reinforced cement composites (FRC). According to these researchers, FRC can be classified as a tensile strain-softening or tensile strain-hardening material. A tensile strain-hardening FRC is always a deflection hardening material, while a tensile strain-softening FRC can have a deflection hardening or softening behavior (Fig. 1).

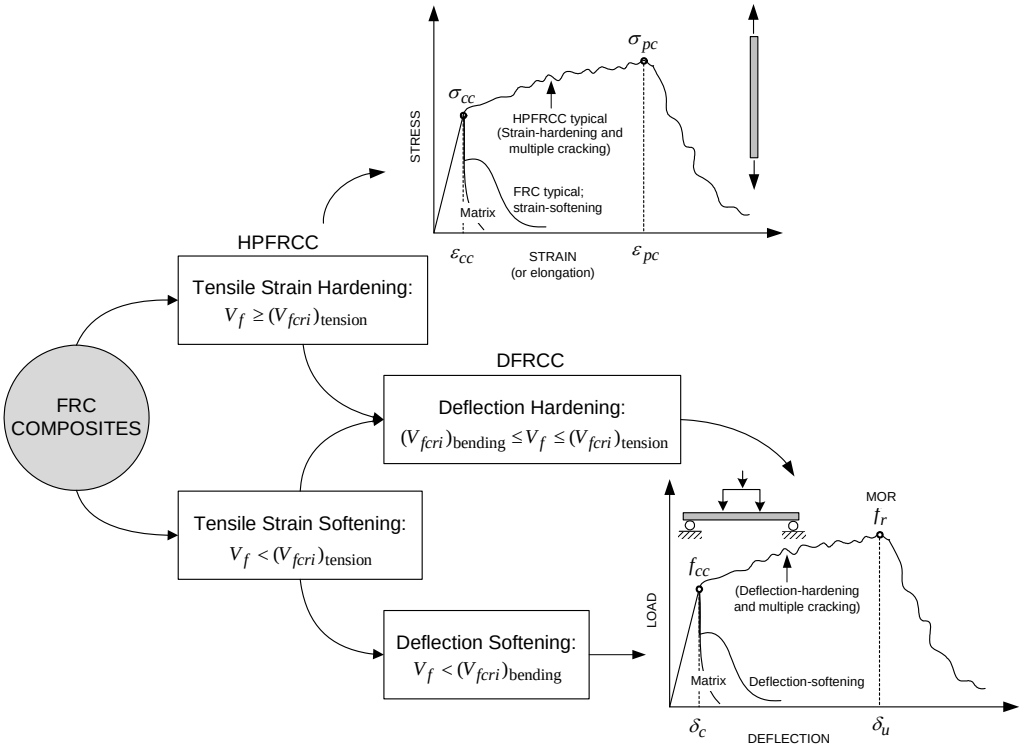

Figure 1. FRC classification [2].

Engineered cementitious composite (ECC) is a tensile strain-hardening material with post-cracking resistance that can be much higher than the stress crack initiation of the matrix, relatively high energy absorption capacity, and durability [3-6]. These unique characteristics of ECC material motivated several researchers to study the applicability of this material in distinct civil engineering situations, being the

strengthening of existing structures one of the elected fields [7, 8]. Test results with reinforced concrete (RC) interior beam-column joints repaired with 15 mm thick ECC jacket confining entirely the joint showed much improved behavior in terms of maximum load, displacement ductility, energy dissipation, and stiffness degradation [9]. The joint shear failure observed in control specimen was transformed into a flexural failure mode in repaired specimens.

Difficulties on assuring enough workability for the ECC to accomplish good filling conditions to cast ECC in place joint impose extra challenge on the development technology of ECC. To overcome these difficulties, a prefabricated ECC panel, designated CARDIFRC, was developed [10, 11]. The tests carried out showed that damaged RC beams can be successfully strengthened and rehabilitated. It was concluded that this technique may be used when there is a need to improve the durability of existing concrete structures, since CARDIFRC mixes are very durable due to their highly dense microstructure. In another study an ECC layer was added to the beams flexural strengthened with FRP system [14]. The results showed that ECC, covering the FRP system, can indeed be used to delay debonding of the FRP, contributing for a more effective use of the FRP material. Other studies related with retrofitting, using cast-in-place steel fiber reinforced cementitious composites (SFRCC), can be found in [13-15]. Recently, twenty one plain concrete beams with pre-defined cracks were prepared and repaired using different combinations of ECC alone or together with CFRP [16]. Researchers found that the repair with ECC was effective in enhancing the member ductility. It was also shown that pasting CFRP directly over ECC substrate resulted in shear failure rather than the undesirable interfacial debonding failure mode that typically occurs in case of concrete substrates. ECC was also able to change the mode of failure of the beams.

Twelve concrete columns retrofitted with externally bonded prefabricated steel fiber reinforced cement composite SFRCC panels (forming a jacket) were recently tested [17]. The main test parameters were the cross-section shape of the original specimens and the thickness of the jackets. Test results showed that both ductility and strength of the specimens increased remarkably due to the introduction of SFRCC jackets.

Since the cost of ECC is higher than of normal concrete due to the use of relatively high contents of fibers and cement, some research efforts are being done combining ECC with RC in order to reduce the overall costs of the strengthening intervention [18, 19]. In this context, two beam-column specimens consisting of RC with an ECC crust were tested. The results of these two tests indicated that the shear capacity of RC

with a thin ECC crust and without shear reinforcement is similar to that of the RC alone but with standard steel stirrup as shear reinforcement.

Currently a new technique of strengthening is under study in the structural division of university of Minho. This technique is based on the use of thin prefabricated panels of ECC that includes fiber reinforced polymers (FRP) sheet glued in the inner surface of the panel. The main aim of this study is examining the advantages of this innovative hybrid system for rehabilitation of existing structures against seismic loadings. In fact, the quasi-rigid plastic behavior of ECC in tension up to the ultimate strain of the FRP systems will be used for the reinforcement of the prefabricated panels.

To this purpose an initial effort to develop a cost-competitive and toughness ECC material has being done and its results are presented in this report.

The minimum requirements of the ECC material to be developed are: compressive strength of at least 30 MPa; Young's modulus between 30 and 35 GPa; stress at crack initiation of about 3 MPa; strain-hardening behavior up to a tensile strain higher than 1.5%. For this strain level the crack pattern should be diffuse and the crack width should not exceed 0.3 mm. To obtain a cost-competitive ECC for the first trial, equal content of cement, fly ash and limestone filler is used. The effect of adding Poly vinyl alcohol (PVA) discrete fibers to the matrix, as reinforcement, in two different percentages is studied.

2 SPECIMEN DETAILS AND PREPARATION

Test specimens consisted of two groups, *ECC1* and *ECC2*. Both groups included twelve similar bending beams but with different content of fibers. Specimens have a prismatic geometry with a length of *160 mm* and cross section of *40x40 mm²* (*Fig. 2*).

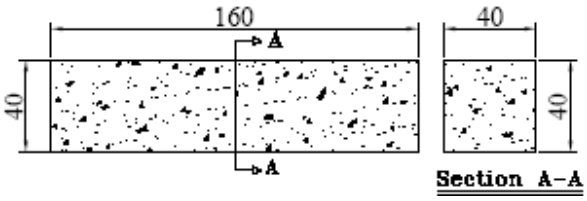

Figure 2. Geometry of used specimens for flexural test (dimensions in mm)

The matrix material is composed of cement, fly ash, limestone filler, fine sand and super-plasticizer (Table 1). PVA fibers in a content of one and two percent in volume of cementitious matrix was used in ECC1 and ECC2, respectively. The mechanical and geometrical properties of PVA fibers used in this study are shown in table 2. During the mix procedure the fibers were added to the matrix very slowly in a tentative

to obtain a homogenous mix composition as possible, especially in the case of ECC2 specimens with two percent of fibers.

Table 1. Mix composition for ECC1 and ECC2 normalized by the binder (Cement + Fly Ash) weight

Mix Components	*Description*	*Density kg/m^3*	*Weight Ratio**
Cement	*I 42.5R*	*3150*	*0.50*
Fly Ash	*Class F*	*2362*	*0.50*
Lime-Stone Filler	*Micro 100AB*	*2700*	*0.50*
Fine Sand	*Max grain size: 1.20 mm*	*2300*	*1.73*
Water	*-*	*1000*	*0.32*
*Super-Plasticizer***	*Sika 3002 HE*	*1060*	*0.009*
*ECC1_PVA-Fibers ****	*Kurary REC 15x8*	*1300*	*0.022*
*ECC2_PVA-Fibers ****	*Kurary REC 15x8*	*1300*	*0.043*

** Weight Ratio = component weight / binder weight ; binder : Cement + Fly Ash*

*** SP: 1.8% of cement weight*

**** PVA-Fibers for ECC1 and ECC2: 1% and 2% of total mix volume respectively*

Table 2. REC15×8 PVA-Fibers Properties

Length (mm)	*Diameter (μm)*	*Tensile Strength (MPa)*	*Elastic Modulus (GPa)*	*Strain Capacity (%)*	*Density (g/cm^3)*
8	*40*	*1560*	*40*	*6.5*	*1.3*

Steel standard moulds for mortar bending test were used. After filling the moulds with the composite material, external vibration was applied with plastic hammer. After have been cured during one day in the laboratory natural environmental conditions, the specimens were removed from the moulds and cured in the water for at least 28 days.

3 TEST PROCEDURES

Experimental tests were carried out to characterize the mechanical properties of ECC materials under flexural and compression.

To determine the flexural tensile strength four specimens of each group were tested under four point loads. A displacement transducer, type of LVDT, was applied in each specimen to measure the deflection of the specimen during testing. An LVDT was also installed in the tensile bottom surface of the specimen to measure the average strain and, indirectly, the average crack width, since the number of cracks in the measuring length of this LVDT was also evaluated at the end of the test (Fig. 3).

Three point (centre-point) flexural tests on notched prisms were also carried out to determine the contribution of the fibers for the post-crack residual strength of the specimens. A notch of 20 mm depth and 3.8 mm width was made in the middle span of the four specimens that compose each group (Fig. 4). An LVDT was attached to a steel bar fixed in the alignments of the supports of the specimen in order to measure the mid span deflection of the specimen. Another LVDT was installed at the lateral face of the specimen, close to the notch tip in order to measure the crack mouth opening displacement (CMOD). This LVDT was mounted on aluminum tabs glued on each side of the notch (Fig. 5b). The results of this type of tests were also used to estimate the fracture energy of the composite material (energy to propagate a crack of unit area), which is designated as mode I fracture energy, and can be an indicator of the ductility of the material. After the prismatic specimens have been tested in bending, cubic specimens of 40 mm edge are extracted from the two lateral parts of the prisms in order to assess the compressive strength of the composite.

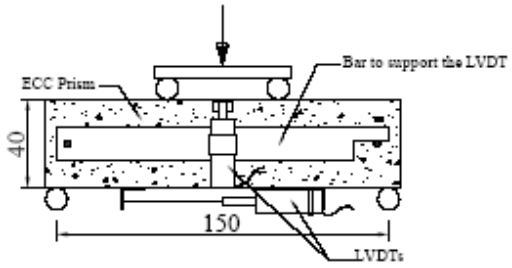

Figure 3. Test setup for four-point bending test using un-notched specimens (dimensions in mm)

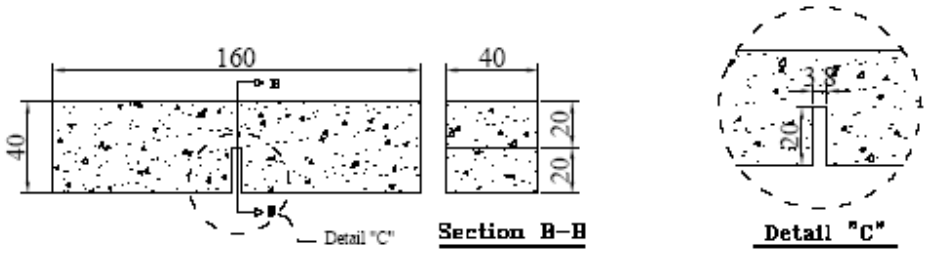

Figure 4. Geometry of the notch of the specimens (dimensions in mm)

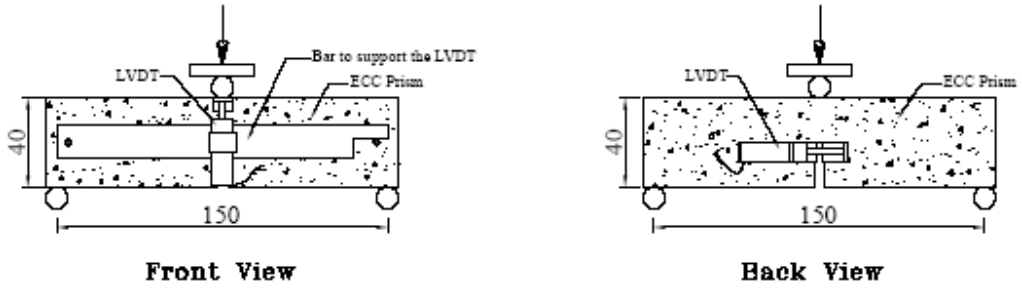

(a) (b)

Figure 5. Test setup for three-point bending test using notched specimens: (a) Front view; (b) Back view (dimensions in mm)

The remaining specimens were used to evaluate the cracking moment and the corresponding deflection by performing three-point bending tests with un-notched specimens. In this case the only measured parameters were the load and the mid span deflection. Test setup is shown in Fig. 6.

The flexural test was controlled through an external LVDT mounted on the actuator, having been adopted a deflection rate of 5 micrometers per second. The vertical deflection was measured by the other LVDT attached to the specimen.

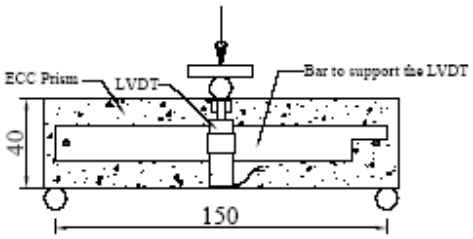

Figure 6. Test setup for three-point bending test using un-notched specimens (dimensions in mm)

4 Discussion of Test Results

4.1 Four Point Bending Test with Un-Notched Specimens

The load-mid span deflection curves for ECC1 and ECC2 specimens are shown in Figs. 7 and 8. The global behavior of all the specimens in both groups is similar. Load-mid span curves are following a deflection hardening phase after linear part and then present a softening phase up to the end of the test. As it is shown is Tables 3 and 4, the average initial flexural stiffness (K_b) for ECC1 and ECC2 is around 109 kN/mm (COV= 7%) and 88.7 kN/mm (COV= 5.8%), respectively, while the average maximum

resisting moment for ECC1 and ECC2 is 165 kN.mm and 173 kN.mm, respectively, that represents an increase of 5%.

In terms of morphology, no more than two cracks were formed in ECC1 specimens, while in ECC2 specimens at least three cracks were observed. For both groups, after the formation of the initial cracks (end of the linear branch) the width of one of the cracks started to increase (localization) while the width of the other cracks had no major visible change. After crack initiation, the part of the load that is mainly carried through the matrix was transferred to the fibers. One could interpret the sudden drops in these curves as the result of the stress transfer process from matrix to the fibers bridging the faces of the cracks. In fact, these drops are due to the sudden release of crack formation energy, but eventual deficiencies on the test control system and test setup configuration can also contribute for this effect. It is possible to reduce the magnitude of this effect with a better test setup, e.g.: controlling the test by the external LVDT attached to the specimen.

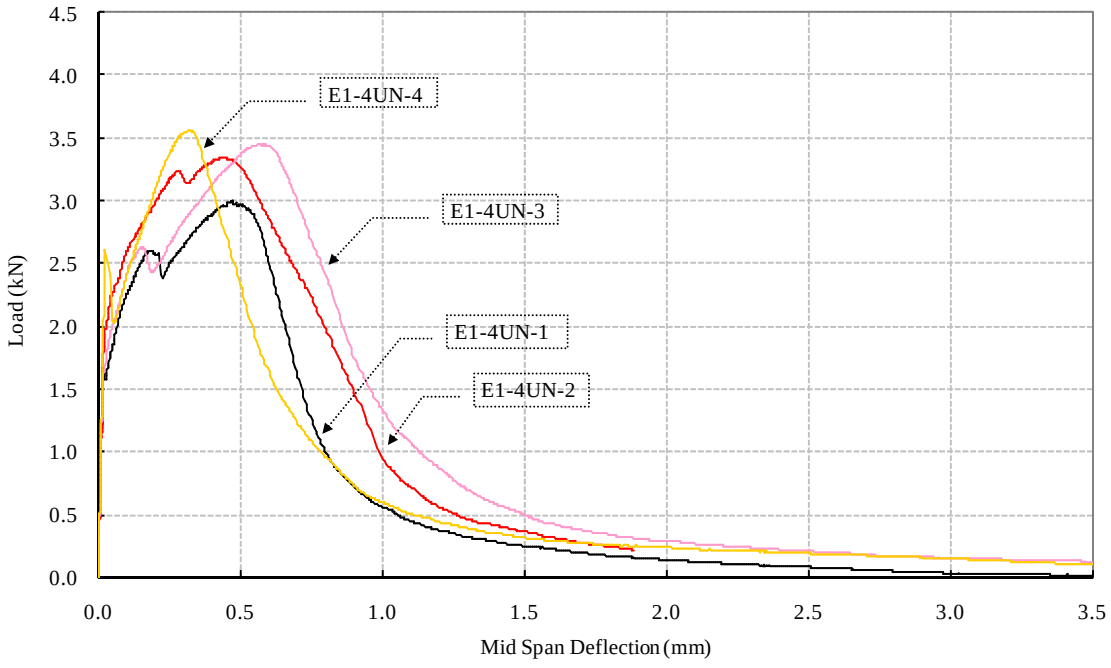

Figure 7. Load-mid span deflection curves of four-point bending ECC1 specimens

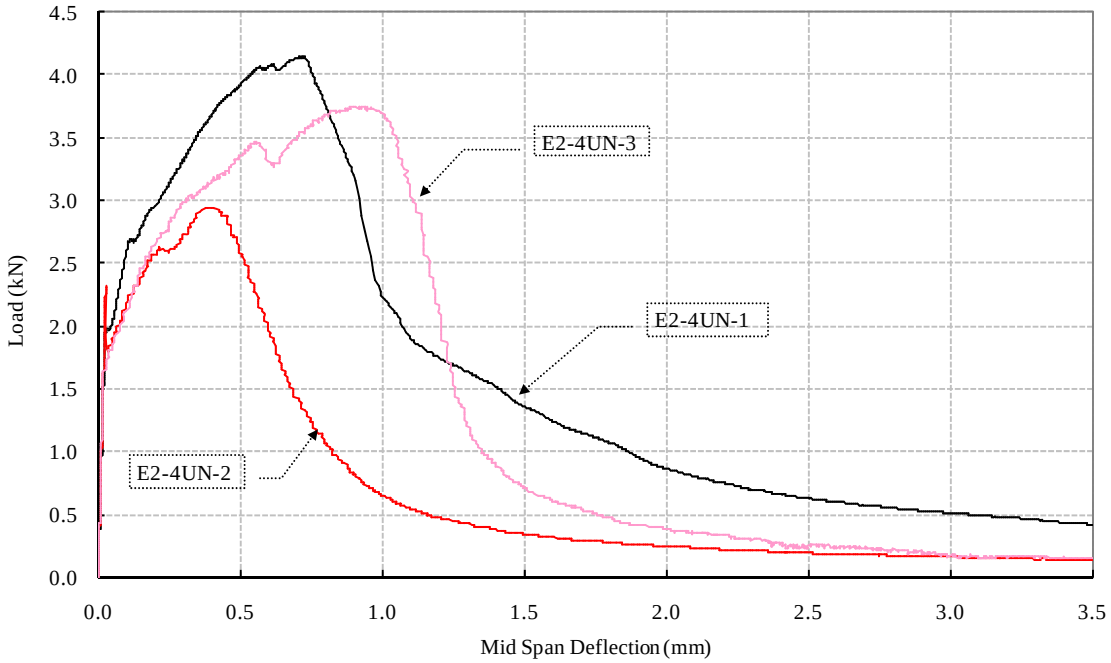

Figure 8. Load-mid span deflection curves of four-point bending ECC2 specimens

(*One specimen was not considered due to its quite abnormal response)

To determine the tensile strength of the developed ECC, the Fib-UHPFRC Ultra high performance fiber reinforced concrete) recommendations are used [20]. According to these recommendations, to evaluate the performance of UHPFRC, the tensile strength is obtained from the force value (F_{fiss}) corresponding to the loss of linearity of the initial elastic phase of the force-deflection curve. The flexural tensile stress (R_{fl}) at crack initiation is calculated using the following equation:

$$R_{fl} = \frac{F_{fiss} l_s^{\,2}}{bh^2} \quad (1)$$

Where l_s is the length of the specimen between supports, and b and h are the width and the height of the specimen cross section.

To estimate the tensile strength, the flexural tensile stress at crack initiation is corrected for the gradient effect. The approach is the same as that recommended by CEB-FIP structural design code [21]:

$$f_{ct,el} = R_{fl} * S_f \quad (2)$$

$$S_f = \frac{2.0 * \left(\frac{h}{h_0}\right)^{0.7}}{1 + 2.0 * \left(\frac{h}{h_0}\right)^{0.7}} = 0.51 \quad with \ h_0 = 100 \ mm$$

Tensile strength ($f_{ct,el}$) values for ECC1 and ECC2 are presented in Tables 3 and 4 respectively. The average values for both specimens are almost the same, around 2.34 MPa.

Elastic modulus of materials was estimated using general relationship between load and mid-span deflection for beams under four-point bending. Ignoring the small deflection due to the self-weight of the beam, the load-deflection relationship for linear elastic range is:

$$\delta_{ms} = \frac{4 \times F \times l_s^3}{243EI} \tag{3}$$

Where F is the total load applied by the actuator, l_s is the length of the specimen between the supports; E is the modulus of elasticity of the matrix; and I is the moment inertia of the cross section.

The average value for elastic modulus of ECC1 and ECC2 specimens are around 28 and 23 GPa, respectively (Tables 3 and 4).

4.2 THREE-POINT BENDING TEST WITH UN-NOTCHED SPECIMENS

In order to estimate the stress at crack initiation, the results of three-point bending tests with un-notched prisms are used (Fig. 9 and 10). The cracking moment, M_{cr}, is obtained from

$$M_{cr} = \frac{F_{cr} \times L}{4} \tag{4}$$

Where F_{cr} is the cracking load, having been assumed as the load when a reduction of 10% in initial secant stiffness occurred. The stress at crack initiation is obtained from:

$$\sigma_{cr} = \frac{M_{cr}}{S_m} \tag{5}$$

Where, S_m is the section flexural modulus.

The calculated values for M_{cr} and σ_{cr} are presented in Tables 5 and 6. As expected, the fibers did not contribute for the σ_{cr}, so identical values were obtained for both groups of tests: 5.48 MPa for ECC1 and 5.23 MPa for ECC2 (only 5% difference).

Table 3. Results of four-point bending test with ECC1 specimens

Specimen designation	F_{fiss} kN	D_{fiss} mm	R_{fl} MPa	$f_{ct,el}$ MPa	K_b kN/mm	E GPa
E1-4UN-1	1.64	0.016	3.85	1.98	117.63	30.63
E1-4UN-2	1.92	0.019	4.50	2.31	99.55	25.93
E1-4UN-3	1.54	0.015	3.60	1.85	107.59	28.02
E1-4UN-4	2.61	0.025	6.11	3.13	111.30	28.98
Average	1.93	0.019	4.52	2.32	109.02	28.39
COV %	24.94	23.72	24.94	24.94	6.93	6.93

Table 4. Results of four-point bending test with ECC2 specimens

Specimen designation	F_{fiss} kN	D_{fiss} mm	R_{fl} MPa	$f_{ct,el}$ MPa	K_b kN/mm	E GPa
E2-4UN-1	1.92	0.023	4.49	2.30	83.14	21.65
E2-4UN-2	2.31	0.026	5.42	2.78	89.80	23.39
E2-4UN-3	1.64	0.018	3.85	1.98	93.21	24.27
Average	1.96	0.02	4.59	2.35	88.72	23.10
COV %	17.23	18.81	17.23	17.23	5.78	5.78

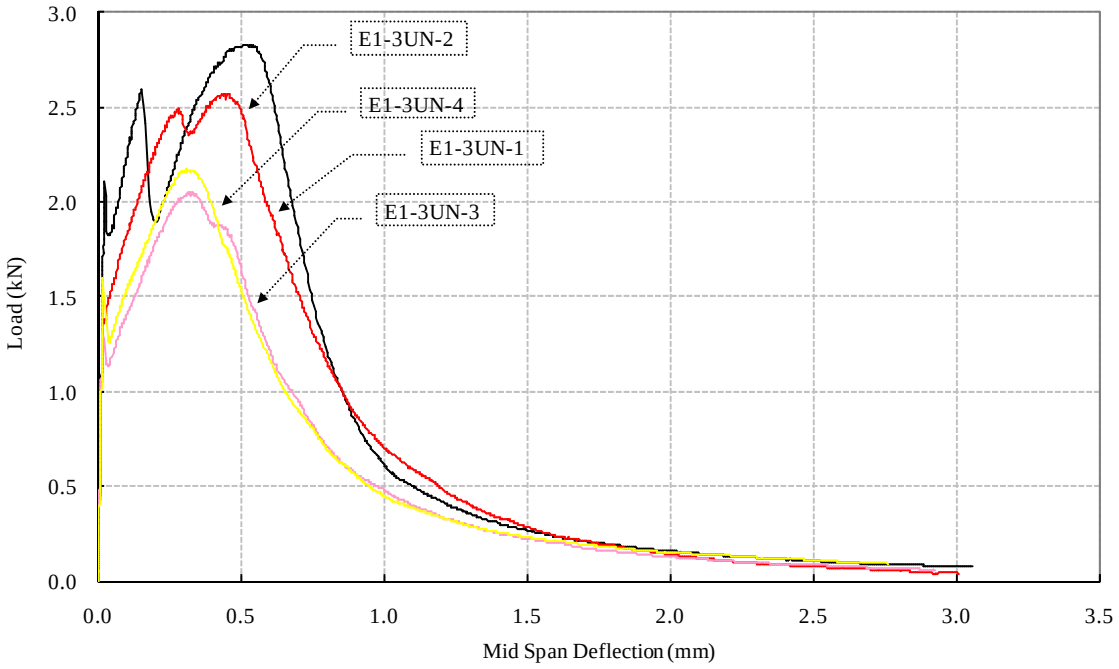

Figure 9. Load-mid span deflection curves of three-point bending ECC1 un-notched specimens

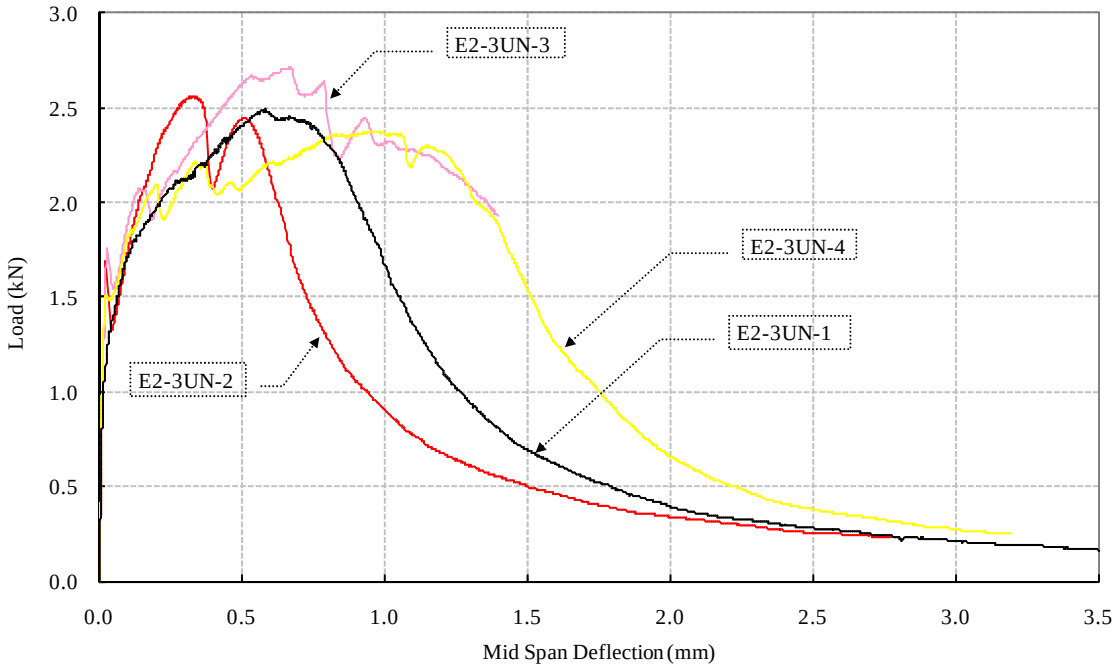

Figure 10. Load-mid span deflection curves of three-point bending ECC2 un-notched specimens

Table 5. Results of center-point bending tests with ECC1 un-notched specimens

Specimens	F_{cr} kN	D_{cr} mm	M_{cr} kN.mm	σ_{cr} MPa
E1-3UN-1	2.07	0.022	77.66	7.28
E1-3UN-2	1.29	0.014	48.30	4.53
E1-3UN-3	1.28	0.014	48.04	4.50
E1-3UN-4	1.60	0.018	60.00	5.63
Average	1.56	0.017	58.50	5.48

Table 6. Results of center-point bending test, ECC2 un-notched specimens

Specimens	F_{cr} kN	D_{cr} mm	M_{cr} kN.mm	σ_{cr} MPa
E2-3UN-1	1.03	0.015	38.70	3.63
E2-3UN-2	1.65	0.023	61.88	5.80
E2-3UN-3	1.76	0.027	65.93	6.18
E2-3UN-4	1.51	0.021	56.51	5.30
Average	1.49	0.022	55.75	5.23

4.3 THREE-POINT BENDING TEST WITH NOTCHED SPECIMENS

RILEM recommendations [21] specify a three-point bending test to characterize the post-cracking behavior of mortar and concrete. The value of the required energy to open the unit area of crack, fracture energy (G_f), can be derived by dividing the area under the load-crack width curve (Figs. 11 and 12) by the area of the fracture surface. Herein two values of fracture energy are evaluated. The first value, designated as G_{f1}, corresponds to the fracture energy dissipated during the pseudo-deflection-hardening phase of the crack propagation process. The value of G_{f1} is the area under the stress-crack with curve, between the first load drop and the initiation of the softening behavior (points P1 and P2 in Figure 11). The other is the energy dissipated up to a crack width of 3.0 mm, herein designated by G_{f2} (Tables 7 and 8). The average value of G_{f1} for ECC1 specimens is 0.14 N/mm, while for ECC2 specimens are 0.18 N/mm, which represents an increase of 30%. An increase around 25% was obtained for G_{f2} when compared the results of ECC2 and ECC1 specimens.

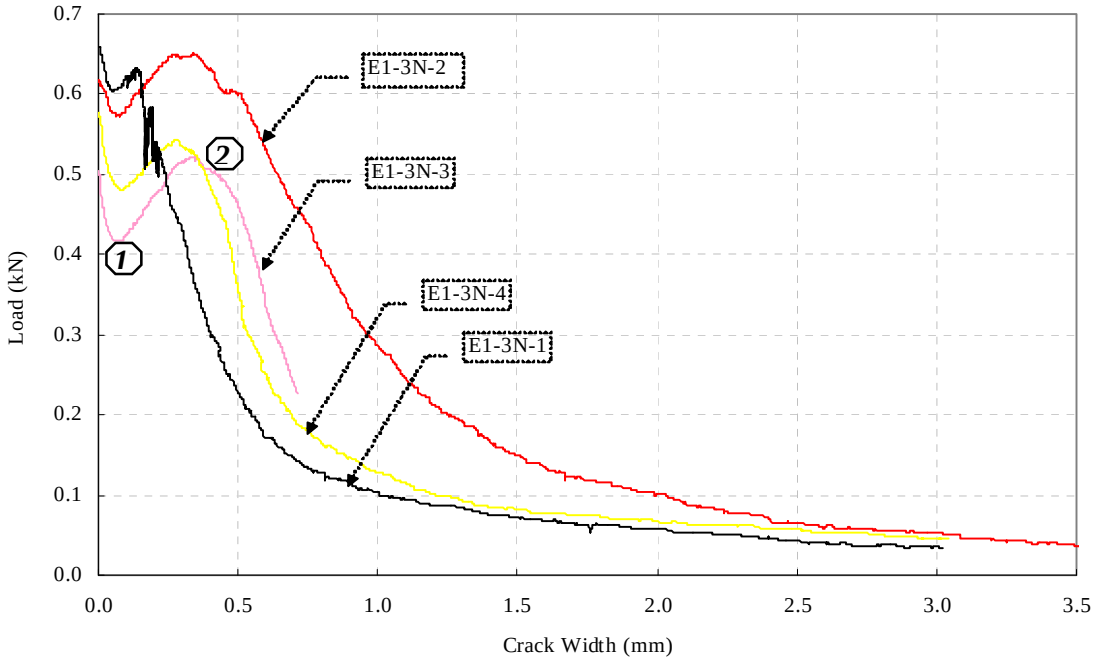

Figure 11. Load- Crack width curves of three-point bending tests with ECC1 notched specimens

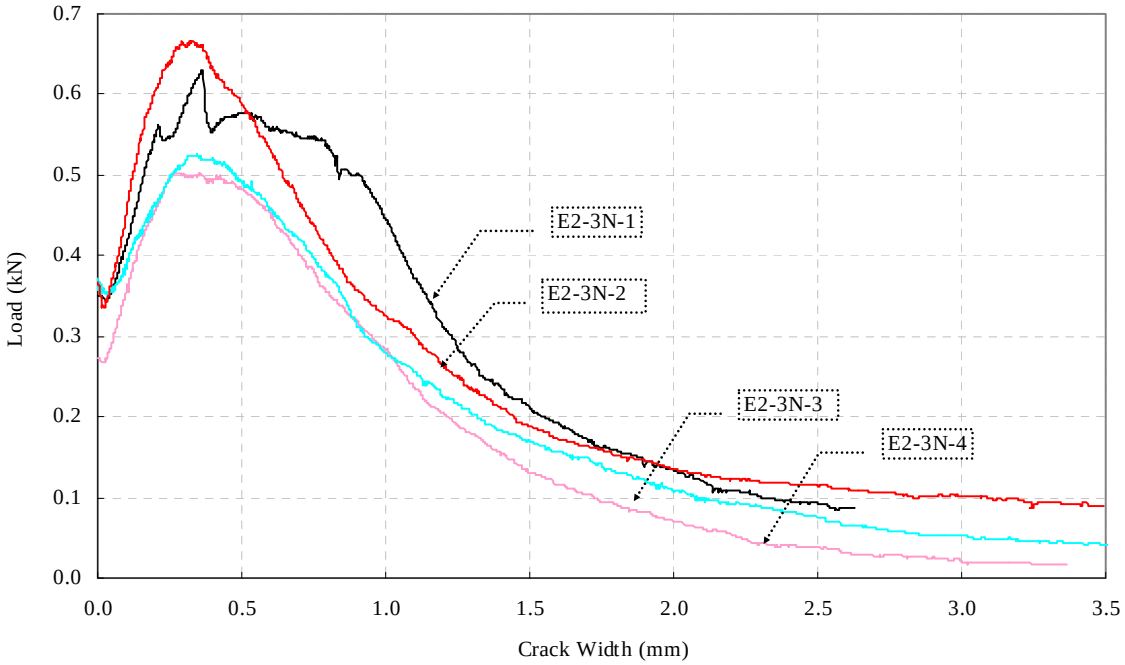

Figure 12. Load- Crack width curves of three-point bending with ECC2 notched specimens

The contribution of fibers in the post-cracking behavior is examined through the residual strength (f_R) at different crack mouth openings [22, 23] (CMOD= 0.5, 1.5, 2.5, 3.0 mm). The obtained results are presented in Table 7 and 8. The average values at different CMODs are much higher in ECC2 specimens than ECC1. For instance, for 0.5 mm crack width the value of f_R for ECC2 specimens are about 24% higher than the corresponding value for ECC1 specimens.

The significant scatter of the values and the high coefficients of variation (COV) for the specimens of each group are the reflex of the random nature of fiber distribution and orientation in the cement medium.

Table 7. Results of three-point bending test withECC1 notched specimens

Specimen designation	*Residual flexural strength, f_R, (MPa) for CMOD (mm)*				*Dissipated Energy (N/mm)*	
	0.5	*1.5*	*2.5*	*3.0*	G_{f1}	G_{f2}
E2-3N-1	*0.249*	*0.072*	*0.043*	*0.035*	*0.063*	*0.53*
E2-3N-2	*0.601*	*0.155*	*0.066*	*0.053*	*0.208*	*0.95*
E2-3N-3	*0.474*	*N/A*	*N/A*	*N/A*	*0.161*	*N/A*
E2-3N-4	*0.411*	*0.084*	*0.059*	*0.047*	*0.129*	*0.61*
Average	*0.434*	*0.104*	*0.056*	*0.045*	*0.140*	*0.70*
COV%	*33.7*	*43.3*	*21.1*	*20.4*	*43.1*	*31.8*

Table 8. Results of three-point bending test width ECC2 notched specimens

Specimen Code	*Residual flexural strength, f_R, (MPa) for CMOD (mm)*				*Dissipated Energy (N/mm)*	
	0.5	*1.5*	*2.5*	*3.0*	*Gf1*	*Gf2*
E2-3N-1	*0.574*	*0.218*	*0.093*	*N/A*	*0.214*	*N/A*
E2-3N-2	*0.595*	*0.190*	*0.115*	*0.102*	*0.207*	*1.03*
E2-3N-3	*0.484*	*0.134*	*0.038*	*0.022*	*0.133*	*0.75*
E2-3N-4	*0.499*	*0.171*	*0.077*	*0.053*	*0.164*	*0.85*
Average	*0.538*	*0.178*	*0.081*	*0.059*	*0.180*	*0.88*
COV%	*10.2*	*19.8*	*40.2*	*68.4*	*21.3*	*16.5*

4.4 COMPRESSIVE STRENGTH

At the end of a three-point bending test with un-notched specimens the end parts of these specimens were cut in order to get cubic samples of an edge of 40 mm. These samples were subjected to

compression loading by using compressive machine for mortar tests. The average value of the compressive strength for ECC1 specimens is about 32% higher than ECC2 (table 9). This indicates that the vibration process to prepare the mix composition for ECC2 was not sufficient enough; therefore a relatively high content of voids remained in the mix. This is why the tensile properties of ECC2 are only marginally higher than those of ECC1, even for a relatively high increase of content of fibers (the double). The failure of the specimens for the two group specimens was completely different. ECC1 specimens failed with a loud sound indicating sudden crush of the cubic (similar to a brittle mortar), while ECC2 specimens presented a much more ductile failure mode.

Table 9. Compressive test Results

Sample Code	*ECC1*		*ECC2*	
	F (kN)	*fc (MPa)*	*F (kN)*	*fc (MPa)*
1	*94.1*	*58.8*	*79.2*	*49.5*
2	*92.3*	*57.7*	*73.6*	*46.0*
3	*106.9*	*66.8*	*73.2*	*45.8*
4	*100.0*	*62.5*	*77.2*	*48.3*
5	*98.4*	*61.5*	*73.0*	*45.6*
6	*97.5*	*60.9*	*70.7*	*44.2*
Average	*98.2*	*61.4*	*74.5*	*46.6*

4.5 SEM ANALYSIS

Producing a material with diffuse cracking able to undergo significant strain hardening during tensile loads was one of the objectives of this research. This kind of material can absorb high amount of energy during hardening phase through the forming of multiple micro cracks before localization. This characteristic is generally described by saturated cracks index. Based on definition of Tjiptobroto and Hansen [24], if the energy needed to form a new crack be less than the energy needed to propagate the crack, then multiple cracking behavior will happen. In order to have a composite with high strain ductility it is necessary to reduce the toughness and first crack initiation of matrix in comparison with complementary energy and maximum bridging capacity of fibers respectively. The results of the current test showed unsatisfactory behavior of the mix composition in terms of multiple cracking. Even there is many factors related to this phenomenon, the performance of interface bond between matrix and fibers is the major one. Two kind of

bond could be defined: chemical and frictional bond [25]. When the interfacial bond is so high it could prevent the full length slippage of the fibers and eventually the process of rupture in fibers will diminish the cracking bridge stresses. To evaluate the global performance of the interface bond the scanning electron microscopy (SEM) was used. It is found that for both ECC1 and ECC2 groups most of fibers ruptured during the test (Fig. 13). Abrasion effects caused by surrounding hard material lead to severe damage in coating of fibers and consequently significant reduction in fibers surface (Fig. 14). Also in some cases the rupture of the fibers was accompanied with delaminating of fibers (Fig 15).

5 CONCLUSIONS AND FUTURE STUDIES

The mix composition for both groups of specimens satisfied some of the minimum desired requirements such as compressive strength, elastic modulus and stress at crack initiation. Even the material exhibited deflection-hardening behavior. However, the developed composites did not present a diffuse crack pattern.

Based on the SEM analysis results it was found that the slip-hardening mechanism, in the fibers-matrix interface was not fully developed due to premature rupture of fibers. This is related to the strong chemical and interfacial bond. Since the chemical bond is an inherent characteristic of interface zone, which is just related to the tailoring of the fibers, coating and interaction with cement paste, in the next trial mix the only alternative is optimizing the frictional bond. To this purpose increasing the amount of the fly ash is recommended. At the same time it is desired to reduce the toughness of the matrix to have a safer margin to develop a strain hardening material. Reducing the size of the sand could effectively change the toughness of matrix.

Using direct tensile test in order to verify directly the strain capacity of the material and categorizing the behavior based on tensile strain hardening or softening is recommended too. In this way a new mix for verification of an innovative mould, designed for direct tensile test, is done. The results of this test are presented in the Annex.

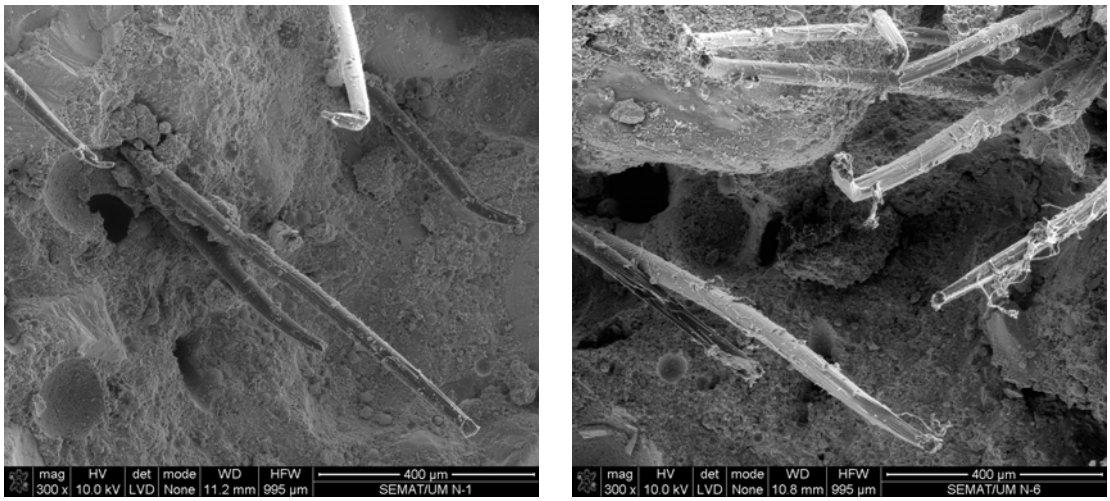

(a) (b)

Figure 13. Fibers' rupture has governed the performance of ECC (a) ECC1; (b) ECC2

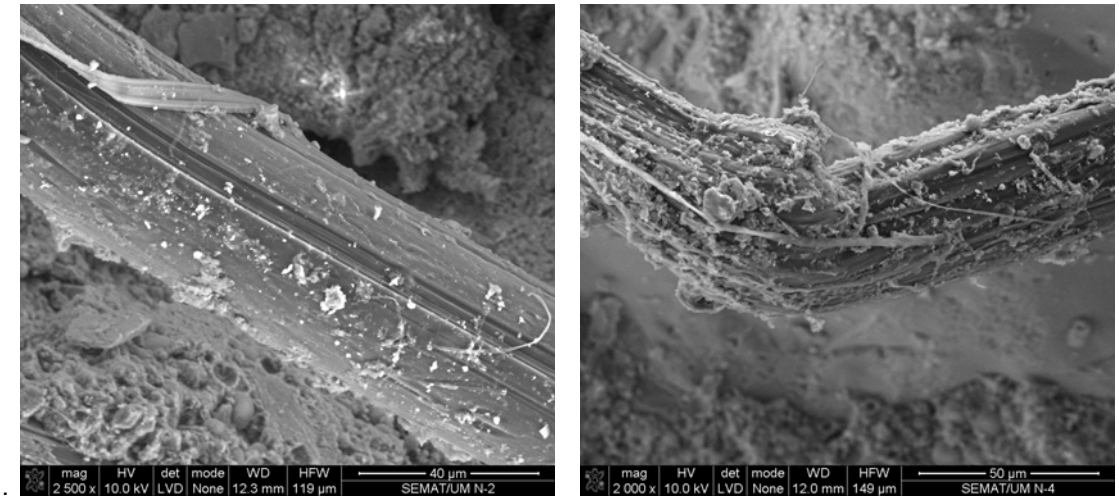

(a) (b)

Figure 14. Abrasion effect of surrounding material destroyed the coating and reduced the surface of fibers (a) ECC1; (b) ECC2

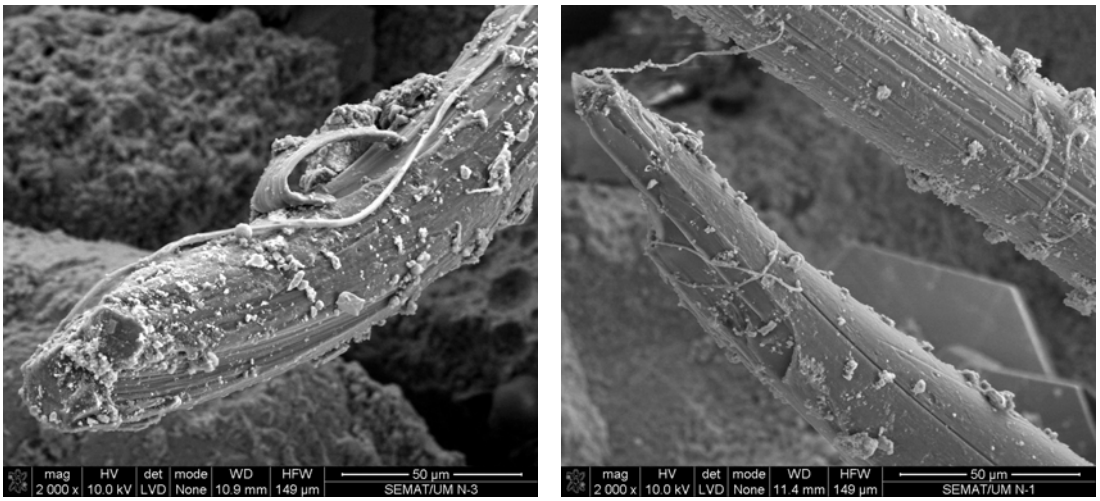

(a) (b)

Figure 15. Delaminating of fibers (a) ECC1; (b) ECC2

6 REFERENCES

[1] Romualdi, J.P., and Mandel, J.A., “Tensile Strength of Concrete Affected by Uniformly Distributed and Closely Spaced Short Lengths of Wire Reinforcement”, ACI Journal, Proceedings, Vol. 61, no.6. June 1964, pp 657-670

[2] Naaman A.E. and Reinhardt H.W., (2003), "High Performance Fiber Reinforced Cement Composites - HPFRCC 4," RILEM Proc., PRO 30, RILEM Pbs., S.A.R.L., Cachan, France; June 2003; 546 pages.

[3] Maalej, M., Hashida, T., and Li, V.C., "Effect of Fiber Volume Fraction on the Off-Crack Plane Energy in Strain-Hardening Engineered Cementitious Composites," Journal of American Ceramics Society, vol.78, no.12, pp.3369-3375, 1995

[4] Li, V.C., Mishra, D.K., Naaman, A.E., Wight, J.K., LaFave, J.M., Wu, H.C., and Inada, Y., "On the Shear Behavior of Engineered Cementitious Composites," J. of Advanced Cement Based Materials, vol.1, no.3, pp.142-149, 1994

[5] Li, V.C. (2003); “On Engineered Cementitious Composites – a review of the material and its applications.”, Journal of Advanced Concrete Technology, 1(3), p. 215-30.

[6] E.B. Pereira, G. Fischer, J.A.O. Barros, M. Lepech “Crack formation and tensile stress-crack opening behavior of Fiber Reinforced Cementitious Composites (FRCC)”, Paper submitted to Francos09, November 2009.

[7] Bank, L.C., Lamanna, A.J., Ray, J.C., and Velazquez, G.I. 2002. Rapid Strengthening of Reinforced Concrete Beams with Mechanically Fastened, Fiber-Reinforced Polymeric Composite Materials. US Army Corps of Engineers. Report Number ERDC/GSL TR-02-4. 93 pages.

[8] Parra-Montesinos, G.J. (2005); “High-Performance Fiber-Reinforced Cement Composites - an alternative for seismic design of structures”, ACI Structural Journal, 1(102), p. 668-675.

[9] Shannag, M.J., Barakat, S., and Abdul-Kareem, M. “Cyclic behavior of HPFRC-repaired reinforced concrete interior beam-column joints”, Materials and Structures/Mat6riaux et Constructions, Vol. 35, pp 348-356, July 2002.

[10] Alaee, F.J., “Retrofitting of Concrete Structures Using High Performance Fibre Reinforced Cementitious Composite (HPFRCC)”, PhD Thesis, Cardiff University, Cardiff, 2002.

[11] Alaee, F.J., and Karihaloo, B.L., “Retrofitting of reinforced concrete beams with CARDIFRC”, Journal of Composites for Construction 7(3), 174-186 ,2003.

[12] Maalej, M., Leong, K.S., “Engineered cementitious composites for effective FRP-strengthening of RC beams”, Composites Science and Technology 65,1120–1128, 2005.

[13] Shannag, M.J., Barakat, S., Jaber F., “Structural repair of shear-deficient reinforced concrete beams using SIFCON”, Magazine of Concrete Research 53(6), 391-403, 2001.

[14] Dogan, E., and Krstulovic-Opara, N., “Seismic retrofit with continuous slurry-infiltrated mat concrete jackets”, ACI Structural Journal 100(6), 713-722, 2003.

[15] Harajli, M.H., and Rteil, A.A., “Effect of confinement using fiber-reinforced polymer or fiber reinforced concrete on seismic performance of gravity load-designed columns”, ACI Structural Journal 101(1), 47-56 ,2004.

[16] Anwar A.M., Hattori, K., Ogata, H., Ashraf, M., and Mandula, “Engineered Cementitious Composites for Repair of Initially Cracked Concrete Beams”, Asian Journal of Applied Sciences 2 (3): 223-231, 2009.

[17] Ilki, A., Akgun, D., Goray, O., Demir, C., and Kumbasar, N, “Retrofit of Concrete Members with Externally Bondded Prefabricated SFRCC Jackets.” M.S. Konsta-Gdoutos, (ed.), Measuring, Monitoring and Modeling Concrete Properties, 625–632, © Springer, Printed in the Netherlands, 2006.

[18] Van Dyk, W .D., “Development of thin fibre reinforced cementious plates and investigating influence of sand on ECC behaviour”, Final year BEng Thesis, University Stellenbosch, South Africa, 2004.

[19] Avenant, P., “Engineered Cement-based composites (ECC) for the application of permanent formwork”, Final year BEng Thesis, University Stellenbosch, South Africa, 2005.

[20] Fib-UHPFRC (Draft6)

[21] RILEM. FMC1 - Determination of the fracture energy of mortar and concrete by means of three-point bend tests on notched beams, Materials and Structures, Vol. 18, No. 106, pp. 285-290, July-August 1985.

[22] RILEM. Technical Committee 162-TDF - Test and design methods for steel fiber reinforced concrete. Recommendation for bending test (Chairlady L. Vandewalle), Materials and Structures, Vol. 33, No. 225, pp. 3-5, January-February 2000.

[23] RILEM. Technical Committee 162-TDF - Test and design methods for steel fiber reinforced concrete. Final Recommendation, Materials and Structures, Vol. 35, pp. 579-582, November 2002.

[24] Tjiptobroto, Prijatmadi and Hansen, Will, “Tensile Strain-hardening and Multiple Cracking in High-Performance Cement-Based Composites Containing Discontinuous Fibers”, ACI Materials Journal, January-February 1993.

[25] Li, V.C., Wu, C., Wang, S., Ogawa, S., and Saito, T., “Interface tailoring for strain-hardening PVA-ECC,” ACI Mater J 99 (5) (2002), pp. 463–472

A.1 ANNEX

In order to verify a new mix design for ECC preparation and also a recommended mould for direct tensile test, an experimental program is performed.

MIX DESIGN

During the process of designing the matrix two main goals was considered: reducing the frictional bond between fibers and matrix to have a slip hardening phase; and reducing the fracture toughness of the matrix to increase the safety margin for developing a tensile strain hardening material in comparison with complementary energy (Fig. 16).

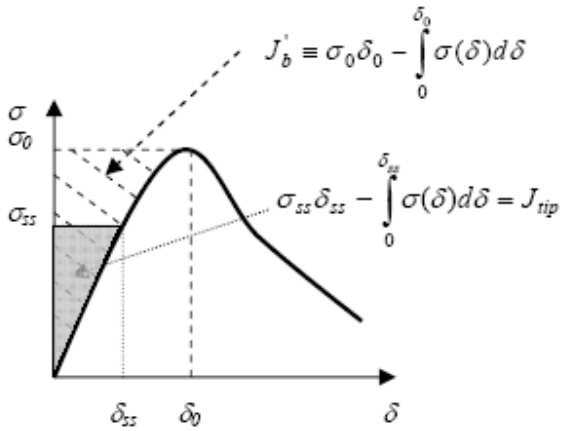

Figure 16. Typical stress-deformation curve for tensile strain-hardening composite. Hatched area represents complimentary energy J'_b. Shaded area represents crack tip toughness J_{tip}.

To reduce frictional bond decreasing the hardness of the interface zone is effective. Using the higher amount of fly ash, this purpose will be achievable. The particles of the fly ash, with the size of microns meters, will have the role of filling of the voids, increasing the workability and, since it has a spherical configuration, the hardness of matrix interface will decrease significantly, leading to a smaller frictional bond performance.

The crack toughness of the matrix is directly related to the size of the sand. Finer sand will represent a lower toughness of the matrix. The mix design is shown in Table 10.

Table 10. Mix composition for ECC2, normalized by the binder (Cement + Fly Ash) weight

Mix Components	*Description*	*Density kg/m^3*	*Weight Ratio**
Cement	*I 42.5R*	*3150*	*0.50*
Fly Ash	*Class F*	*2362*	*0.50*
Fine Sand	*Max grain size: 0.50 mm*	*2300*	*0,33*
Water	*-*	*1000*	*0,26*
Super-Plasticizer	*Gelnium 77 SCC*	*1060*	*0,0094*
Viscosity modifier agent	*RHEOMATRIX 100*	*1020*	*0,0014*
*PVA-Fibers ***	*Kurary REC 15x8*	*1300*	*0,02*

** Weight Ratio = component weight / binder weight ; binder : Cement + Fly Ash*

*** PVA-Fibers is 2% of total mix volume*

EXPERIMENTAL TEST

The experimental tests are composed of direct tensile test on two notched samples and three point bending test on two notched small beams.

DIRECT TENSILE TEST

To prepare specimens for direct tensile test a new mould was designed. The main idea of this mould was to force the concentration of fibers in planar dispersion in a gradually reduced section zone (Fig 17). Using this sample, the behavior of a single crack bridged by fibers could be easily assessed. Two small notches are introduced on both sides of the specimens to force the formation of a single crack.

An LVDT of a measuring length of 50 mm is used to control the test at a displacement rate of 0.017 micron per minutes. Test setup is shown in Fig. 18.

THREE-POINT BENDING TEST

Three point bending test is performed on two notched prisms. The geometry and the test setup are same as shown before in figures 3 and 4. The only difference is that the flexural test was controlled through an external LVDT which is attached to a steel bar fixed in the alignments of the supports of the specimen. The test for specimen one performed with a deflection rate of 5 micrometers per second, while this value reduced to 1 micron in the test of the specimen two.

TEST RESULTS

The tensile test shows a strain hardening behavior with a strain capacity up to an average strain of 0.61 mm/mm. The first crack strength for specimen one (ECC2_T1) was around 3.75 MPa while this value for the second specimen was 2.14 MPa. The average ultimate tensile strength of two specimens is almost the same and around 5 MPa (Fig. 19). During the test for both specimens more than one crack formed close to the notched zone. This indicates the need of lower notch thickness to have just single crack for future experiments (Fig. 20).

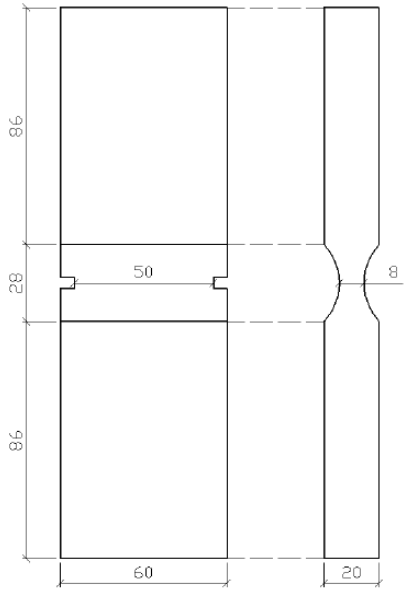

Figure 17. Specimens geometry for direct tensile test

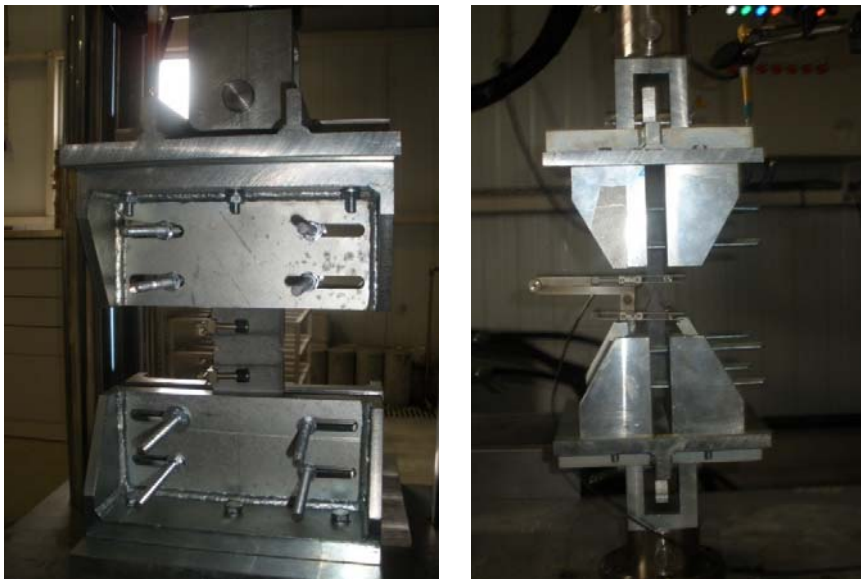

(a) (b)

Figure 18. Direct tensile test setup a) Front View; b) Side view

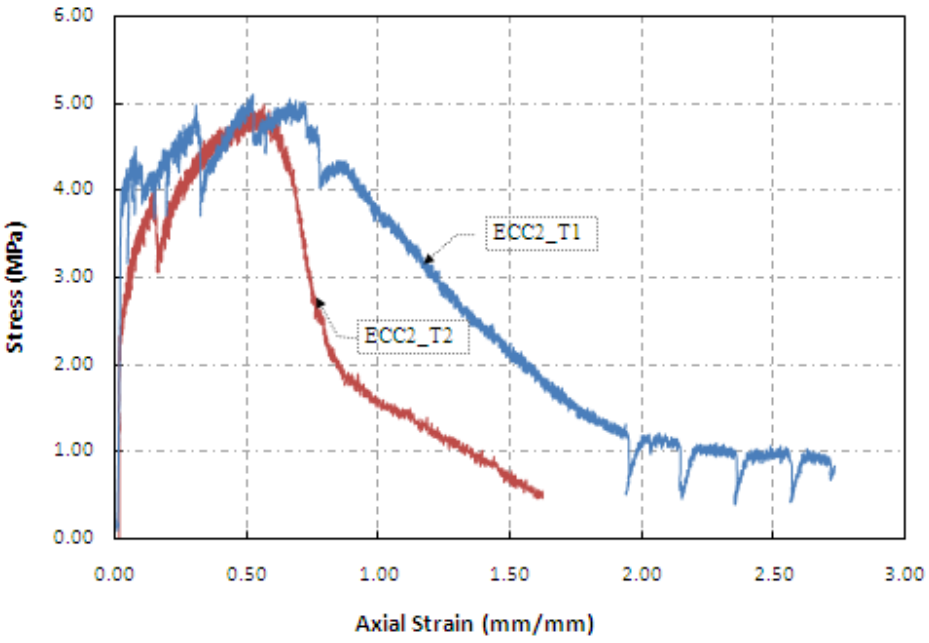

Figure 19. Tensile stress – strain curve for ECC2

(a)

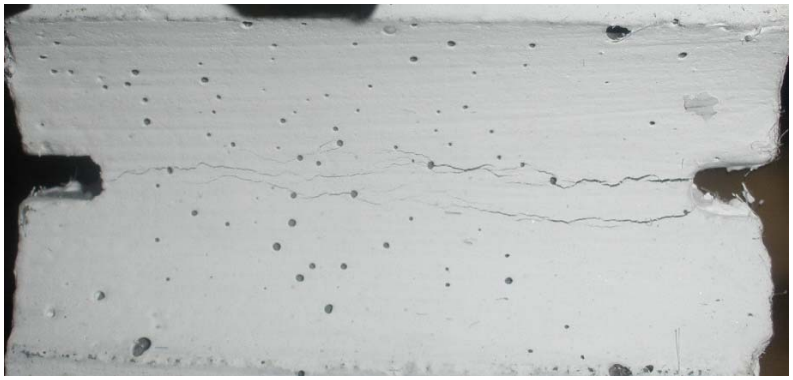

(b)

Figure 20. Formation of multiple cracks close to the notched zone a) specimen ECC_T1; b) specimen ECC_T2.